Title

Neuropilin-2 promotes lineage plasticity and progression to neuroendocrine prostate cancer.

Journal

Oncogene, 41(37)

Authors

Wang, Jing
Li, Jingjing
Yin, Lijuan
et al.

Publication Date

2022-09-01

DOI

10.1038/s41388-022-02437-0

Peer reviewed

HHS Public Access

Author manuscript

Oncogene. Author manuscript; available in PMC 2023 March 01.

Neuropilin-2 Promotes Lineage Plasticity and Progression to Neuroendocrine Prostate Cancer

Jing Wang[1,*], **Jingjing Li**[1,*,#], **Lijuan Yin**[2,$], **Tianjie Pu**[1], **Jing Wei**[1], **Varsha Karthikeyan**[3,4], **Tzu-Ping Lin**[5,6], **Allen C. Gao**[7], **Boyang Jason Wu**[1]

[1]Department of Pharmaceutical Sciences, College of Pharmacy and Pharmaceutical Sciences, Washington State University, Spokane, WA 99202, USA

[2]Uro-Oncology Research Program, Samuel Oschin Comprehensive Cancer Institute, Department of Medicine, Cedars-Sinai Medical Center, Los Angeles, CA 90048, USA

[3]Summer Undergraduate Research Fellowship Program, College of Pharmacy and Pharmaceutical Sciences, Washington State University, Spokane, WA 99202, USA

[4]Department of Integrative Biology, School of Life Sciences, College of Science, Oregon State University, Corvallis, OR 97331, USA

[5]Department of Urology, Taipei Veterans General Hospital, Taipei, Taiwan 11217, Republic of China

[6]Department of Urology, School of Medicine and Shu-Tien Urological Research Center, National Yang-Ming University, Taipei, Taiwan 11221, Republic of China

[7]Department of Urologic Surgery, University of California Davis, Sacramento, CA 95817, USA

Abstract

Neuroendocrine prostate cancer (NEPC), a lethal subset of prostate cancer, is characterized by loss of AR signaling and resulting resistance to AR-targeted therapy during neuroendocrine transdifferentiation, for which the molecular mechanisms remain unclear. Here, we report that neuropilin 2 (NRP2) is upregulated in both *de novo* and therapy-induced NEPC, which induces neuroendocrine markers, neuroendocrine cell morphology and NEPC cell aggressive behavior. NRP2 silencing restricted NEPC tumor xenograft growth. Mechanistically, NRP2 engages in reciprocal crosstalk with AR, where NRP2 is transcriptionally inhibited by AR, and in turn suppresses AR signaling by downregulating the AR transcriptional program and confers resistance

Correspondence: Boyang Jason Wu, Washington State University, 205 E Spokane Falls Blvd, PBS 421, Spokane, WA 99202, USA. Phone: 509-368-6691; Fax: 509-368-6561; boyang.wu@wsu.edu.
[#]Present address: Laboratory of Regeneromics, School of Pharmacy, Shanghai Jiao Tong University, Shanghai 200240, China
[$]Present address: Department of Pathology, West China Hospital, Sichuan University, Chengdu, Sichuan 610041, China
[*]These authors contributed equally to this work

Author Contributions

B.J.W. conceived the study. J. Wang, J.L., and B.J.W. designed the experiments. J. Wang, J.L., L.Y., T.P. J. Wei, and V.K. performed the experiments. J. Wang, J.L., L.Y., and B.J.W. analyzed the data. T-P.L. provided human CRPC tissue microarrays. A.C.G. provided control and ENZ^{R} C4-2B cells. B.J.W. wrote the manuscript, supervised the study and acquired funding.

Conflict of Interest statement: The authors declare that they have no conflict of interest.

Supplementary Information

Supplementary information includes 6 supplementary figures, 2 supplementary tables, supplementary materials and methods, and supplementary references.

to enzalutamide. Moreover, NRP2 physically interacts with VEGFR2 through the intracellular SEA domain to activate STAT3 phosphorylation and subsequently SOX2, thus driving NEPC differentiation and growth. Collectively, these results characterize NRP2 as a driver of NEPC and suggest NRP2 as a potential therapeutic target in NEPC.

Introduction

Prostate cancer (PC) is the second most frequent cancer and the fifth leading cause of cancer death in men worldwide [1]. Androgen deprivation therapy (ADT) is the mainstay treatment for PC. Although ADT is initially effective, the majority of tumors relapse with castration-resistant characteristics (CRPC), a subset of which further develop small-cell or neuroendocrine (NE) features (NEPC) [2, 3]. With the introduction of highly potent antiandrogen drugs such as enzalutamide (ENZ) for CRPC management, the incidence of therapy-induced NEPC has been escalating in recent years. Although it rarely occurs *de novo*, NEPC has been reported in up to 25% of advanced therapy-resistant CRPC patients [2]. NEPC demonstrates high proliferative rates and reduced/lost androgen receptor (AR) signaling, resulting in resistance to AR-targeted therapy, and currently has no effective treatment [4].

Recent studies indicate that the molecular pathogenesis of NEPC involves orchestrated genetic alterations, epigenetic reprogramming and microenvironmental cues for activation of a range of master transcriptional regulators, oncogenic signaling pathways and cellular events associated with lineage switch to promote NE differentiation [5]. Despite these discoveries, the molecular mechanisms controlling NEPC development and progression still remain unclear.

Neuropilins (with 2 homologs, NRP1 and NRP2) are broadly expressed multifunctional transmembrane proteins that bind to vascular endothelial growth factors (VEGFs) and class 3 semaphorins as their coreceptors to regulate vascular development and axon guidance, respectively. Neuropilins are frequently overexpressed in many human tumors, including PC, and demonstrate the ability to regulate tumor growth and progression [6, 7]. Several studies have revealed NRP2 upregulation in human PC adenocarcinoma, correlated with increasing Gleason grade and shorter cancer-specific survival [8, 9]. NRP2 expression has been recently shown to be further elevated in bone metastatic PC adenocarcinoma compared to primary or metastatic PC adenocarcinomas from other sites [10]. Despite these findings, little is known about neuropilin expression and function in NEPC. This study explored the role and mechanism of NRP2 in NEPC.

Results

NRP2 expression is upregulated in NEPC

To seek NRP2's clinical relevance to aggressive PC variants, we evaluated NRP2 expression in a tissue panel of primary PC, CRPC and NEPC by immunohistochemistry (IHC). We found higher NRP2 levels in human CRPC and NEPC compared to primary PC. NRP2 levels were further elevated in NEPC with pure small-cell/NE histology compared to CRPC

(Fig. 1A). Examining *NRP2* expression in publicly available RNA-seq datasets, we showed that *NRP2* mRNA levels were upregulated in hormone-refractory tumors (HRPC) compared to hormone-sensitive tumors (HSPC) (GSE6752), and in NEPC patient-derived xenografts (PDXs) compared to adenocarcinoma (Adeno) PDXs (GSE32967 and GSE66187) (Fig. 1B). Using the NE marker CHGA for assessing NE differentiation in CRPC tumors, we found a positive correlation between NRP2 and CHGA protein expression in a CRPC tissue microarray (Fig. 1C). We also demonstrated a positive mRNA co-expression correlation between *NRP2* and two NE markers, *ENO2* and *NCAM1*, in 5 independent PC cohorts (DKFZ 2018 [11], TCGA, SMMU 2017 [12], MSKCC 2010 [13], and Broad/Cornell 2012 [14]) (Fig. 1D). *NRP2* mRNA further demonstrated a positive correlation with NEPC score based on a set of 70 NEPC reference genes [15] in the SU2C/PCF 2019 mCRPC cohort [16] (Fig. 1E). Additionally, gene set enrichment analysis (GSEA) of genes differentially expressed in *NRP2*-high relative to *NRP2*-low PC patient samples from the TCGA cohort showed similar transcriptomic profiles to NEPC, including 285 genes overexpressed and 180 genes underexpressed in NEPC [15, 17, 18] (Fig. 1F).

To determine NRP2's association with NE characteristics in human PC cells, we measured *NRP2* expression across different human PC cell lines. *NRP2* expression remained marginal prevalently in AR^{+}/NE^{-} cell lines (LAPC4, LNCaP, C4–2 and C4–2B) and rose toward an increasing NE degree (Fig. 1G). *NRP2* expression was the highest in the AR^{-} *de novo* small-cell/NE NCI-H660 cells [19] and second highest in the AR^{-}/NE-like PC-3 cells with reported characteristics of prostatic small-cell/NE carcinoma [20]. We also detected moderate *NRP2* levels in 22Rv1 cells with dual AR/NE positivity [21, 22].

To examine NRP2 expression in therapy-induced NEPC, we used an ENZ-resistant (ENZ^{R}) C4–2B ($C4–2B^{ENZR}$) cell line, which recapitulates the clinical transition of CRPC to NEPC under ADT [23]. We demonstrated upregulated NRP2 expression in $C4–2B^{ENZR}$ cells compared to controls, paralleled by reduced AR and PSA expression and enhanced levels of several NE markers (CHGA, CD56, NSE, SYP and SOX2) (Fig. 1H). We also performed GSEA with the RNA-seq data from $C4–2B^{ENZR}$ and control cells (GSE159548) and demonstrated significant enrichment of the gene signatures related to neuropilin binding, defined as binding to a member of the neuropilin family in the GO database, as well as NRP2 targets in $C4–2B^{ENZR}$ cells compared to controls (Fig. 1I). The NRP2 targets were defined as the top 100 differentially expressed genes ranked by fold change in absolute value ($p<0.001$) in NRP2-knockdown relative to control $C4–2B^{ENZR}$ cells by RNA-seq (Supplementary Table 1). We also found that $C4–2B^{ENZR}$ cells were enriched for the gene signatures of angiogenesis and axon guidance, where NRP2 plays an active role (Fig. 1I). Additionally, we interrogated a dataset (GSE70380) from a patient progressing on ADT and found higher *NRP2* mRNA levels post 12-week ENZ treatment, paralleled by increased and reduced levels of *NCAM1* and *KLK3* respectively (Fig. 1J). Collectively, these results indicated NRP2 upregulation in NEPC.

NRP2 is suppressed by androgen signaling

To examine whether AR ablation activates NRP2 in NEPC, we treated LNCaP and C4–2B cells, which both express NRP2 but with a higher level in C4–2B than LNCaP as

demonstrated by us (Supplementary Fig. 1) and others [9, 10], with ENZ. We found that ENZ time-dependently increased *NRP2* mRNA levels along with reduced *KLK3* levels in a 7-day observation period (Fig. 2A). Analysis of RNA-seq data (GSE8702) from LNCaP cells grown in androgen-deprived medium for up to 11 months demonstrated time-dependent increases of *NRP2* and *ENO2* mRNA levels (Fig. 2B). Next, we treated LNCaP cells with ENZ for 6 hours, which led to activation of *NRP2* and *ENO2* mRNA with a concomitant *KLK3* decrease (Fig. 2C). Conversely, treatment of LNCaP and C4–2B cells with the synthetic androgen R1881 for 6 hours caused a reduction in *NRP2* mRNA levels along with increased *KLK3* and decreased *ENO2* levels (Fig. 2D). These findings suggest that *NRP2* expression may be transcriptionally suppressed by AR.

To explore whether AR binds to the *NRP2* gene locus, we interrogated two ChIP-seq datasets involving LNCaP cells (GSE161167) and human prostate tissues (GSE70079). We initially identified two AR-bound regions residing in *NRP2* introns 7 and 15 respectively, but we were only able to validate AR interaction with the sequence encompassing the ChIP-seq AR peak in intron 15, not intron 7, in R1881-treated LNCaP cells by chromatin-immunoprecipitation (ChIP)-qPCR assays (Supplementary Fig. 2). Thus, we decided to focus on the AR-bound intron 15 hereafter. In the LNCaP cells, the affinity of AR association with intron 15 was boosted upon dihydrotestosterone (DHT) treatment. In the clinical samples, higher AR occupancy at intron 15 was shown in most tumor tissues relative to normal prostate tissues. Further, we identified a consensus androgen response element (ARE, +89,311~+89,325) within the AR-bound intronic sequence, which has high homology with the canonical ARE sequence GGT/AACAnnnTGTTCT [24] (Fig. 2E). To validate AR occupancy at this ARE, we conducted ChIP-qPCR assays and revealed AR occupancy at the ARE-centric sequence upon R1881 stimulation, paralleled by minimal AR binding in the absence of R1881. A sequence of *NRP2* exon 1 as a negative control demonstrated no AR occupancy regardless of R1881 treatment (Fig. 2F). To determine whether the identified ARE was functional, we inserted the corresponding ARE-centric sequence upstream of the minimal promoter-driven luciferase gene to construct a *NRP2* ARE-luc reporter. Compared with the WT *NRP2* ARE-luc inductive to ENZ at 6 hour, mutations of select nucleotides in the ARE made the reporter no longer responsive to ENZ in LNCaP cells (Fig. 2G)

To seek the clinical relationship of NRP2 with AR, we demonstrated a negative correlation between *NRP2* mRNA versus AR score defined by assessment of 30 AR target genes in the SU2C/PCF 2019 cohort (Fig. 2H), corroborated by the negative mRNA co-expression correlations of *NRP2* with several AR target genes in 4 independent cohorts (Fig. 2I). Analysis of the CRPC samples in the Grasso 2012 cohort [25] indicated an inverse relationship of *NRP2* mRNA with serum PSA levels (Fig. 2J). Together, these results suggest that *NRP2* is transcriptionally suppressed by AR, likely via AR binding to a *NRP2* intronic ARE.

NRP2 is necessary to maintain the NE traits and aggressive behavior of NEPC cells

To assess the requirement of NRP2 to support a NE phenotype in PC cells, we stably knocked down NRP2 using two separate shRNAs in C4–2B^{ENZR} and PC-3 cells that both

exhibit NE traits [20, 23]. Validated knockdown of NRP2 reduced protein expression of the NE markers CHGA and CD56 in C4–2B^{ENZR} and PC-3 cells compared to controls (Fig. 3A), accompanied by decreases in a panel of additional NE genes in NRP2-knockdown relative to control C4–2B^{ENZR} cells by RNA-seq-based transcriptomic profiling analysis (Supplementary Fig. 3A and Supplementary Table 2). NRP2 knockdown also resulted in a dedifferentiated cell morphology, a measure of a NE-like phenotype [23], in C4–2B^{ENZR} cells, with decreases in per-cell number of neurites and average neurite length compared to controls (Fig. 3B). Notably, NRP2 knockdown switched the NE lineage of C4–2B^{ENZR} cells back to an AR^{+} luminal cell lineage acquired by prostate adenocarcinoma cells, as evidenced by activation of AR, PSA, two AR pioneer factors involved in positioning AR on chromatin (FOXA1 and GATA2), and several classical AR target genes (*KLK3*, *KLK2* and *TMPRSS2*) (Supplementary Figs. 3B and 3C).

To determine whether NRP2 regulates the aggressive biology of NEPC cells, we found that NRP2 knockdown suppressed C4–2B^{ENZR} and PC-3 proliferation and anchorage-independent colony formation of cells compared to controls (Figs. 3C and 3D). Re-expression of NRP2 into NRP2-knockdown C4–2B^{ENZR} cells restored the proliferation and colony formation to the levels of control cells (Supplementary Figs. 3D and 3E). Concordantly, NRP2 knockdown had similar effects on the proliferation of two additional NE-like PC cell lines, 22Rv1 and NE1.8 (Supplementary Fig. 3F). The NE1.8 cells derived from the LNCaP cell line after long-term ADT develop NE differentiation [26, 27] and express higher NRP2 levels compared to LNCaP cells (Supplementary Figs. 3G). Considering NRP2's anti-apoptotic role in other types of cancer such as colorectal cancer [28], we also examined NRP2's effect on cell apoptosis and found that NRP2 knockdown resulted in significant increases in Annexin V^{+} cell populations, indicative of enhanced cell apoptosis comprising both early and late apoptotic stages, in C4–2B^{ENZR} and PC-3 cells compared to controls (Fig. 3E). Given that NEPC can develop from prostate adenocarcinoma cells after acquiring stem-like properties under ADT [5], we further examined NRP2's effect on stemness and showed that NRP2 knockdown limited tumorsphere establishment by an average of 92% fewer C4–2B^{ENZR} cell spheres compared to controls (Fig. 3F). Collectively, we concluded that NRP2 is essential for maintaining NEPC differentiation and cell behavior.

NRP2 represses AR signaling and promotes NE plasticity

To investigate NRP2's role inducing a NE phenotype in prostate adenocarcinoma cells, we stably overexpressed *NRP2* encoding the NRP2a isoform in LNCaP and 22Rv1 cells, where 22Rv1 also expresses AR-V7, an AR splice variant with ligand-independent constitutive activity [29]. Enforced expression of NRP2 reduced protein expression of AR, AR-V7, PSA, FOXA1 and GATA2 in LNCaP and 22Rv1 cells compared with controls (Fig. 4A). Consistent with these findings, NRP2 overexpression decreased expression of several AR target genes and the activity of an AR-dependent luciferase reporter (*PSA*-luc) in LNCaP and 22Rv1 cells compared with controls (Figs. 4B and 4C). On the other hand, NRP2 overexpression heightened the levels of several canonical NE markers, including CHGA, NSE and SOX2 by Western blot and surface CD56 by flow cytometry, in LNCaP and 22Rv1 cells compared with controls (Figs. 4A and 4D). The reprogramming transcription factor SOX2 was previously reported to promote lineage plasticity during NEPC development

associated with loss of luminal cell identity [30]. In accord with this, NRP2 overexpression led to downregulation of luminal cell markers AR and CK8 in LNCaP and 22Rv1 cells compared with controls (Fig. 4A). Similarly, NRP2 overexpression also repressed AR expression/activity and induced SOX2 expression in C4–2B cells (Supplementary Figs. 4A and 4B).

To examine the biological consequences of NRP2 activation on PC cell behavior, we demonstrated that NRP2 overexpression accelerated the proliferation, anchorage-independent colony formation and tumorsphere formation of LNCaP, 22Rv1 and C4–2B cells compared with controls (Figs. 4E–4G and Supplementary Figs. 4C–4E). We also showed that NRP2 overexpression caused decreases in apoptosis of LNCaP and C4–2B (Fig. 4H and Supplementary Fig. 4F) but not 22Rv1 cells (data not shown), suggesting NRP2-induced cell apoptosis in a cell context-dependent manner. Additionally, we demonstrated that NRP2-overexpressing LNCaP and C4–2B cells displayed androgen-independent cell proliferation with comparable relative fold changes of proliferation rates under ENZ versus vehicle treatment over a 5-day observation period, in contrast to control cells that had a notable reduction in relative fold changes of proliferation rates when exposed to ENZ (Fig. 4I and Supplementary Fig. 4G). Altogether, these results suggest that NRP2 drives NE plasticity for transitioning prostate adenocarcinoma cells to NEPC.

NRP2 induces NEPC through the VEGFR2/STAT3/SOX2 pathway

To search for potential candidate pathways driving NRP2-dependent aggressive NEPC cell behavior, we performed an unbiased proteomic screen using a phospho-kinase array containing 45 phosphosite-specific antibodies to detect 39 proteins involved in the major signaling pathways that regulate cell survival and proliferation. We compared the levels of these signaling phosphoproteins in NRP2-knockdown C4–2B^{ENZR} and NRP2-overexpressing 22Rv1 cells with control cells. The screen nominated STAT3 as the top candidate protein downstream of NRP2 because of its relatively larger phosphoprotein-level change consistent in both cell pairs compared to others. Intriguingly, Y705 is more responsive than S727 to NRP2 (Fig. 5A) likely due to that S727 phosphorylation as a secondary event after Y705 phosphorylation has less responsiveness to stimuli [31], which led us to use Y705 as the measure of STAT3 protein phosphorylation hereafter. Notably, STAT3 was demonstrated to be capable of promoting the aggressive behavior and NE differentiation in PC cells [32, 33]. We confirmed reduced STAT3 phosphoprotein levels in NRP2-knockdown C4–2B^{ENZR} cells alongside increased phosphoprotein levels of STAT3 in NRP2-overexpressing LNCaP, 22Rv1 and C4–2B cells compared to controls by Western blots (Fig. 5B and Supplementary Fig. 4H). We also showed that NRP2 overexpression enhanced the activity of a STAT3-dependent luciferase reporter (SIE-luc) in LNCaP and 22Rv1 cells (Fig. 5C), corroborated by decreased expression of several STAT3 target genes in NRP2-silenced C4–2B^{ENZR} cells, compared to controls (Fig. 5D).

Then we sought to investigate how NRP2 induces STAT3. Since NRP2 is not able to phosphorylate STAT3 by itself due to the deficiency of a kinase function, we hypothesized that NRP2 may partner with other types of proteins, such as receptor tyrosine kinases (RTKs), to activate STAT3. Neuropilins act as coreceptors for several VEGF ligands and

interact with VEGF receptors (VEGFRs) such as VEGFR1 and VEGFR2 to promote endothelial cell survival and migration [34, 35]. Given that PC cells strongly express VEGRF2 and lack VEGFR1 expression [9, 36], we speculated whether NRP2 enhances STAT3 protein phosphorylation via VEGFR2. VEGFR2 expression has been shown in human PC tissues, with its upregulation further seen in advanced-stage compared to early-stage samples [37, 38]. Further, GSEA revealed *VEGFR2* expression in PC patient samples from the TCGA cohort to be highly correlated with genes that are differentially expressed in NEPC (Supplementary Fig. 5A). We demonstrated reduced phosphoprotein levels of VEGFR2 in NRP2-knockdown C4–2B^{ENZR} cells and increased VEGFR2 protein phosphorylation in NRP2-overexpressing LNCaP, 22Rv1 and C4–2B cells compared to controls (Fig. 5E, 5F and Supplementary Fig. 4H). Moreover, we carried out *in situ* proximity ligation assays to visualize an endogenous NRP2-VEGFR2 protein complex, a mechanism NRP2 utilizes to lower the activation threshold of VEGFR2 for more efficient VEGFR2 induction [39]. The NRP2-VEGFR2 interaction was found to be lessened in NRP2-knockdown C4–2B^{ENZR} cell and enhanced in NRP2-overexpressing 22Rv1 cells compared to controls (Fig. 5G). To determine the ligand(s) mediating NRP2-VEGFR2 interaction, we screened the VEGF ligands known to bind to NRP2 and VEGFR2 and found VEGF-A to be the ligand most stably detected and highly enriched in PC cell conditioned media, with its secretion increasing in 22Rv1 and C4–2B^{ENZR} cells compared to LNCaP cells (Supplementary Fig. 5B). We further showed that inhibition of VEGF-A by a neutralizing antibody dose-dependently blocked NRP2-VEGFR2 interaction in C4–2B^{ENZR} cells (Supplementary Fig. 5C). To determine whether VEGFR2 mediates NRP2's effect on STAT3, we showed that NRP2-induced STAT3 protein phosphorylation was reversed upon VEGFR2 knockdown in 22Rv1 cells (Fig. 5H). Neuropilins have been shown to modulate the RTK-downstream signaling of VEGFR2 by binding a neuropilin cytoplasmic motif called SEA, representing the three intracellular C-terminal amino acids serine-glutamic acid-alanine, to the neuropilin-interacting protein GIPC1 [40, 41]. We generated a mutant *NRP2* expression construct with specific removal of the SEA motif (NRP2-ΔSEA) and found that NRP2-ΔSEA failed to induce STAT3 protein phosphorylation in 22Rv1 cells, in contrast to increased levels of STAT3 phosphoprotein caused by WT NRP2 (Fig. 5I). These results suggest NRP2 activation of STAT3 in a VEGFR2-dependent manner.

To further determine whether STAT3 mediates the NRP2-driven aggressive growth and NE traits of NEPC cells, we showed that pharmacologic inhibition of STAT3 by niclosamide [42] suppressed the proliferation of NE-like NRP2-overexpressing LNCaP and C4–2B cells but had a minimal effect on the proliferation of control cells (Fig. 6A and Supplementary Fig. 4I). We also found that knockdown of STAT3 or its upstream activator VEGFR2 reverted the NRP2-induced NE lineage back to an AR^{+} luminal cell lineage by repressing NE markers (CD56 and SOX2) and restoring CK8, AR, PSA, FOXA1 and GATA2 to the levels of controls in LNCaP cells (Supplementary Figs. 6A and 6B). To investigate how STAT3 is mechanistically linked to NRP2-induced NE properties, we performed STRING analysis [43] and identified SOX2 as the primary hub integrating indirect interactions of STAT3 with multiple NE markers and drivers (Fig. 6B), where SOX2 was well characterized as a NEPC master regulator [30, 44]. Following this clue, we demonstrated that inactivation of STAT3 by siRNA or niclosamide attenuated NRP2-induced SOX2 protein expression in

22Rv1 cells (Fig. 6C). STAT3 has been demonstrated as a transcription factor recruited to the *SOX2* promoter to regulate *SOX2* transcription in mouse neural precursor cells and human breast and lung cancer cells [45–47]. To define the STAT3-SOX2 regulatory pattern in NEPC cells, we found that STAT3 occupancy at a known STAT3-bound *SOX2* promoter region was enhanced in NRP2-overexpressing 22Rv1 cells and lessened in NRP2-knockdown C4–2B^{ENZR} cells compared to controls (Fig. 6D). Moreover, we showed that STAT3 knockdown suppressed *SOX2* mRNA expression and promoter activity in NRP2-overexpressing 22Rv1 cells, which was mirrored by a rescue experiment where expression of a constitutively active form of STAT3 (STAT3C) restored *SOX2* mRNA levels and promoter activity in NRP2-knockdown C4–2B^{ENZR} cells (Fig. 6E and 6F). We further demonstrated that siRNA or niclosamide-mediated silencing of STAT3 and SOX2 individually repressed NRP2-induced *NCAM1* expression in 22Rv1 cells (Fig. 6G), suggesting STAT3 and SOX2 as effectors conferring NRP2 action on NE differentiation. Additionally, We found a positive correlation between NRP2 and SOX2 protein expression in the above-used CRPC tissue microarray (Fig. 6H), corroborated by higher *SOX2* mRNA levels in *NRP2*-high compared with *NRP2*-low patient samples from both the TCGA and Beltran 2016 CRPC/NEPC [15] cohorts (Fig. 6I). Collectively, these results support the notion that NRP2 drives NEPC acquisition of aggressive growth and NE marker expression through the VEGFR2/STAT3/SOX2 pathway.

NRP2 silencing inhibits NEPC tumor growth in mice

To address whether NRP2 supports NEPC tumor behavior *in vivo*, we established a PC-3 prostate tumor xenograft mouse model using the doxycycline (Dox)-inducible shRNA expression system. We generated two separate Dox-dependent inducible *NRP2* shRNA expression constructs (shNRP2#1 and shNRP2#2) and stably expressed them individually in PC-3 cells. We observed notable reductions of NRP2 protein expression and cell proliferation upon Dox stimulation consistently across two shRNAs, validating the efficacy of induced NRP2 knockdown (Figs. 7A and 7B). Next, we implanted PC-3 cells stably expressing Dox-inducible *NRP2* shRNA (shNRP2#1) into male immunocompromised mice to form subcutaneous xenografts. One week after inoculation when most mice developed palpable tumors, mice were randomized into two groups and given either a Dox-containing (Dox+) diet or a normal (Dox−) diet. Mice fed with a Dox+ diet leading to induced NRP2 knockdown formed fewer tumors (7/12) compared to control mice receiving a Dox- diet (12/12) (Fig. 7C). Strikingly, Dox-induced tumor NRP2 silencing nearly halted the growth of PC-3 tumors, accompanied by smaller tumor weights at the endpoint, compared to control mice (Figs. 7D–7F). By characterizing tumor samples, we demonstrated lower NRP2 protein expression in Dox-treated tumors compared to controls, indicating effective and sustainable NRP2 knockdown *in vivo* (Fig. 7H). We also found a 75% drop of Ki-67^{+} cells for reduced mitotic index while a roughly 7-fold increase of cleaved caspase 3^{+} cells for enhanced tumor cell apoptosis in NRP2-knockdown tumors compared to controls (Figs. 7G and 7H). NRP2 silencing further reduced CHGA, CD44, phospho-STAT3 and SOX2 protein expression in tumors compared to controls (Fig. 7H). Together, these results suggest the requisite role of NRP2 in supporting NEPC tumor growth in mice.

In summary, our preclinical studies demonstrate that NRP2 is necessary and sufficient for NEPC development and progression. Mechanistically, NRP2 is upregulated upon relieving AR transcriptional repression during NE differentiation, and in turn suppresses AR signaling while activating the VEGFR2/STAT3/SOX2 pathway to induce NE plasticity and the aggressive biology of NEPC cells (Fig. 7I).

Discussion

In this study, we identified NRP2 as a driver of NEPC and defined a NRP2-dependent mechanism conferring a lineage switch of prostate adenocarcinoma cells towards a NE phenotype. Previous studies have well demonstrated NRP2 upregulation in primary and metastatic prostate adenocarcinoma [8–10] where the AR axis is considered active. Here, we presented evidence of continual elevation of NRP2 expression in NEPC clinical samples, a disease stage developed from adenocarcinoma upon long-term and/or more potent inhibition of the AR axis. Our data would be strengthened by including more NEPC samples with pure small-cell/NE histology to increase the sample size for comparisons, though this type of samples is rarely procured in the clinic. Nevertheless, our results and those of others support a notion that NRP2 tends to be highly expressed in both adenocarcinoma and NE prostate tumors.

We demonstrated that NRP2 is transcriptionally suppressed by AR, likely via direct AR interaction with an intronic ARE, leading to NRP2 upregulation in NEPC where AR is in general absent or inhibited. This finding was consistent with the scenario for AR control of the other neuropilin isoform, NRP1, which is transcriptionally repressed by AR binding to AREs within the distal and intron 12 genomic regions of *NRP1* [48]. Our identification of the *NRP2* intronic ARE that can bind to and respond to AR would imply involvement of a DNA looping mechanism whereby the ARE and *NRP2* promoter are brought together through AR and likely other proteins (e.g., an AR-repressive complex) as speculated for the functional intronic AREs found at the genomic loci of other genes [48–51]. To prove this, we interrogated published Hi-C datasets using LNCaP cells (GSE73785 and GSE125640) to examine the predicted DNA looping within the *NRP2* gene locus using *NRP1* that harbors a reported intronic ARE [48] as a positive control. Surprisingly, we did not see the expected chromatin interactions between the ARE-encompassing introns and promoters of both *NRP2* and *NRP1* (data not shown), which we argue could be possibly due to limited data resolution provided by Hi-C assays that were originally designed for exploring large-scale genomic confirmations [52–54]. Thus, further Hi-C/3C analyses achieving sufficient coverage and supporting higher data resolution (e.g., <40 kb) will be required to measure specific small-scale interactions within a subset of the genome well enough to establish the *NRP2* promoter-intron looping facilitated by AR. Reciprocally, we demonstrated that overexpression of the NRP2a isoform inhibits AR expression and transcriptional activity to confer the loss of AR^+ luminal cell identity with concomitant induction of NE features. Interestingly, Dutta *et al.* recently observed that NRP2b, the other isoform of NRP2, can translocate to the inner nuclear membrane to form a complex with AR and nucleoporins and enhance AR transactivation function [55]. Given these discrepancies, we argue that NRP2 may have the dual role of maintaining an AR-repressive state in AR-indifferent NEPC as well as amplifying AR effects in AR-dominant CRPC in an isoform-dependent

manner, which expands the therapeutic utility of targeting NRP2 for treatment of advanced PC, especially for the clinically emergent type of amphicrine tumors composed of cells exhibiting both AR and NE activity [56].

Mechanistically, our results showed that NRP2 induces the VEGFR2/STAT3/SOX2 pathway to drive NEPC differentiation and growth following diminished AR activity and dependence. Our data further point out the requirement of VEGF-A in maintaining NRP2-VEGFR2 interaction and support a ligand-dependent mode of NRP2 action activating VEGFR2 to trigger STAT3 phosphorylation in the NEPC context. In addition to VEGF ligands, NRP2 also functions as a coreceptor to plexins in response to semaphorin ligands such as SEMA3F [57]. Interestingly, NRP2 has been shown to reduce the phosphorylation levels of STAT3 after complexing with SEMA3F and PlexinA1in lung cancer cells [58], suggesting that NRP2 may regulate STAT3 in a ligand- and/or cell context-dependent manner.

In conclusion, our study reveals a NRP2-dictated molecular mechanism controlling a NE lineage switch driving the emergence and progression of NEPC, and proposes targeting NRP2 as a potential therapeutic strategy to treat or prevent NEPC.

Materials and Methods

Clinical specimens

The primary PC tissue microarray PR483c (n=39) in Fig. 1A was obtained from US Biomax. The CRPC tissue microarrays (n=21) in Figs. 1A, 1C and 6H were constructed by the Biobank of Taipei General Veterans Hospital. This study was reviewed and approved by the IRB of Taipei General Veterans Hospital, and written informed consent was provided for patients. The NEPC single section slides (n=4) with pure small-cell/NE histology in Fig. 1A were provided by Dr. Mahul Amin at Cedars-Sinai Medical Center.

Animal studies

All animal studies received prior approval from the IACUC of Washington State University and complied with IACUC recommendations. Male 4- to 6-week-old NSG mice were purchased from Jackson Laboratory and housed in the animal research facility at Washington State University. To determine NRP2's effect on NEPC tumor development and growth, 1×10^6 PC-3 cells expressing Dox-inducible *NRP2* shRNA were mixed 1:1 with Matrigel (BD Biosciences) for bilateral subcutaneous injection into NSG mice. One week after tumor inoculation, mice were randomly divided into two groups (6 mice/group with 2 injection points/mouse) and fed a diet with 625 mg/kg Dox (Dox+, Envigo) or a normal diet (Dox−) *ad libitum*. Tumor size was measured every 2–3 days by caliper after Dox administration. Tumor volume was calculated as length × width^2 × 0.52.

RNA-seq and gene set enrichment analysis

The total RNA of control and NRP2-knockdown C4–2B^{ENZR} cells were extracted by RNeasy Mini Kit (Qiagen) and underwent DNase digestion following the manufacturer's instructions. RNA-seq was performed on an Illumina HiSeq 4000 at Novogene. Bowtie 2 v2.1.0 was used for mapping to the human genome hg19 transcript set. RSEM v1.2.15 was

used to calculate the count and estimate the gene expression normalization. The RNA-seq raw data are available at GEO with the accession number GSE207598. GSEA v4.0.3 was used to evaluate the enrichment of different gene sets from the molecular signature database (MSigDB v7.2) or curated based on related studies.

Statistics

Data are presented as the mean ± SEM as indicated in figure legends. Comparisons between Kaplan-Meier curves were determined using the log-rank test. Correlations were determined by Pearson correlation. All other comparisons were analyzed by unpaired 2-tailed Student's *t* test. A *p* value less than 0.05 was considered statistically significant. Sample size as indicated in figure legends were chosen based on the power to detect significant differences ($p<0.05$) between any experimental and control groups. The investigators were not blinded to the group allocation and outcome assessment during the experiments.

Supplementary Material

Refer to Web version on PubMed Central for supplementary material.

Acknowledgements

This work was supported by Department of Defense Prostate Cancer Research Program grant W81XWH-19–1-0279, NIH/NCI grant R37CA233658, and WSU startup funding to B.J.W. We thank Yidi Xu (Washington State University) for providing technical assistance, Mahul Amin (Cedars-Sinai Medical Center) for providing NEPC clinical samples, and Gary Mawyer for editorial assistance.

References

1. Sung H, Ferlay J, Siegel RL, Laversanne M, Soerjomataram I, Jemal A et al. Global Cancer Statistics 2020: GLOBOCAN Estimates of Incidence and Mortality Worldwide for 36 Cancers in 185 Countries. CA: a cancer journal for clinicians 2021; 71: 209–249. [PubMed: 33538338]
2. Aparicio A, Logothetis CJ, Maity SN. Understanding the lethal variant of prostate cancer: power of examining extremes. Cancer discovery 2011; 1: 466–468. [PubMed: 22586648]
3. Beltran H, Tomlins S, Aparicio A, Arora V, Rickman D, Ayala G et al. Aggressive variants of castration-resistant prostate cancer. Clinical cancer research : an official journal of the American Association for Cancer Research 2014; 20: 2846–2850. [PubMed: 24727321]
4. Wang HT, Yao YH, Li BG, Tang Y, Chang JW, Zhang J. Neuroendocrine Prostate Cancer (NEPC) progressing from conventional prostatic adenocarcinoma: factors associated with time to development of NEPC and survival from NEPC diagnosis-a systematic review and pooled analysis. Journal of clinical oncology : official journal of the American Society of Clinical Oncology 2014; 32: 3383–3390. [PubMed: 25225419]
5. Davies AH, Beltran H, Zoubeidi A. Cellular plasticity and the neuroendocrine phenotype in prostate cancer. Nature reviews Urology 2018; 15: 271–286. [PubMed: 29460922]
6. Ellis LM. The role of neuropilins in cancer. Molecular cancer therapeutics 2006; 5: 1099–1107. [PubMed: 16731741]
7. Rizzolio S, Tamagnone L. Multifaceted role of neuropilins in cancer. Curr Med Chem 2011; 18: 3563–3575. [PubMed: 21756227]
8. Borkowetz A, Froehner M, Rauner M, Conrad S, Erdmann K, Mayr T et al. Neuropilin-2 is an independent prognostic factor for shorter cancer-specific survival in patients with acinar adenocarcinoma of the prostate. International journal of cancer Journal international du cancer 2020; 146: 2619–2627. [PubMed: 31509606]

9. Goel HL, Chang C, Pursell B, Leav I, Lyle S, Xi HS et al. VEGF/neuropilin-2 regulation of Bmi-1 and consequent repression of IGF-IR define a novel mechanism of aggressive prostate cancer. Cancer discovery 2012; 2: 906–921. [PubMed: 22777769]
10. Polavaram NS, Dutta S, Islam R, Bag AK, Roy S, Poitz D et al. Tumor- and osteoclast-derived NRP2 in prostate cancer bone metastases. Bone Res 2021; 9: 24. [PubMed: 33990538]
11. Gerhauser C, Favero F, Risch T, Simon R, Feuerbach L, Assenov Y et al. Molecular Evolution of Early-Onset Prostate Cancer Identifies Molecular Risk Markers and Clinical Trajectories. Cancer cell 2018; 34: 996–1011 e1018. [PubMed: 30537516]
12. Ren S, Wei GH, Liu D, Wang L, Hou Y, Zhu S et al. Whole-genome and Transcriptome Sequencing of Prostate Cancer Identify New Genetic Alterations Driving Disease Progression. European urology 2018; 73: 322–339. [PubMed: 28927585]
13. Taylor BS, Schultz N, Hieronymus H, Gopalan A, Xiao Y, Carver BS et al. Integrative genomic profiling of human prostate cancer. Cancer cell (Research Support, N.I.H., Extramural Research Support, Non-U.S. Gov't) 2010; 18: 11–22. [PubMed: 20579941]
14. Barbieri CE, Baca SC, Lawrence MS, Demichelis F, Blattner M, Theurillat JP et al. Exome sequencing identifies recurrent SPOP, FOXA1 and MED12 mutations in prostate cancer. Nature genetics 2012; 44: 685–689. [PubMed: 22610119]
15. Beltran H, Prandi D, Mosquera JM, Benelli M, Puca L, Cyrta J et al. Divergent clonal evolution of castration-resistant neuroendocrine prostate cancer. Nature medicine 2016; 22: 298–305.
16. Abida W, Cyrta J, Heller G, Prandi D, Armenia J, Coleman I et al. Genomic correlates of clinical outcome in advanced prostate cancer. Proceedings of the National Academy of Sciences of the United States of America 2019; 116: 11428–11436. [PubMed: 31061129]
17. Cheng S, Yu X. Bioinformatics analyses of publicly available NEPCa datasets. American journal of clinical and experimental urology 2019; 7: 327–340. [PubMed: 31763364]
18. Tsai HK, Lehrer J, Alshalalfa M, Erho N, Davicioni E, Lotan TL. Gene expression signatures of neuroendocrine prostate cancer and primary small cell prostatic carcinoma. BMC Cancer 2017; 17: 759. [PubMed: 29132337]
19. van Bokhoven A, Varella-Garcia M, Korch C, Johannes WU, Smith EE, Miller HL et al. Molecular characterization of human prostate carcinoma cell lines. The Prostate 2003; 57: 205–225. [PubMed: 14518029]
20. Tai S, Sun Y, Squires JM, Zhang H, Oh WK, Liang CZ et al. PC3 is a cell line characteristic of prostatic small cell carcinoma. The Prostate 2011; 71: 1668–1679. [PubMed: 21432867]
21. Huss WJ, Gregory CW, Smith GJ. Neuroendocrine cell differentiation in the CWR22 human prostate cancer xenograft: association with tumor cell proliferation prior to recurrence. The Prostate 2004; 60: 91–97. [PubMed: 15162375]
22. Sramkoski RM, Pretlow TG 2nd, Giaconia JM, Pretlow TP, Schwartz S, Sy MS et al. A new human prostate carcinoma cell line, 22Rv1. In vitro cellular & developmental biology Animal 1999; 35: 403–409. [PubMed: 10462204]
23. Bland T, Wang J, Yin L, Pu T, Li J, Gao J et al. WLS-Wnt signaling promotes neuroendocrine prostate cancer. iScience 2021; 24: 101970. [PubMed: 33437943]
24. Roche PJ, Hoare SA, Parker MG. A consensus DNA-binding site for the androgen receptor. Molecular endocrinology 1992; 6: 2229–2235. [PubMed: 1491700]
25. Grasso CS, Wu YM, Robinson DR, Cao X, Dhanasekaran SM, Khan AP et al. The mutational landscape of lethal castration-resistant prostate cancer. Nature (Research Support, N.I.H., Extramural Research Support, Non-U.S. Gov't Research Support, U.S. Gov't, Non-P.H.S.) 2012; 487: 239–243. [PubMed: 22722839]
26. Xu X, Huang YH, Li YJ, Cohen A, Li Z, Squires J et al. Potential therapeutic effect of epigenetic therapy on treatment-induced neuroendocrine prostate cancer. Asian journal of andrology 2017; 19: 686–693. [PubMed: 27905327]
27. Zhang XQ, Kondrikov D, Yuan TC, Lin FF, Hansen J, Lin MF. Receptor protein tyrosine phosphatase alpha signaling is involved in androgen depletion-induced neuroendocrine differentiation of androgen-sensitive LNCaP human prostate cancer cells. Oncogene 2003; 22: 6704–6716. [PubMed: 14555984]

28. Gray MJ, Van Buren G, Dallas NA, Xia L, Wang X, Yang AD et al. Therapeutic targeting of neuropilin-2 on colorectal carcinoma cells implanted in the murine liver. J Natl Cancer Inst 2008; 100: 109–120. [PubMed: 18182619]
29. Hu R, Dunn TA, Wei S, Isharwal S, Veltri RW, Humphreys E et al. Ligand-independent androgen receptor variants derived from splicing of cryptic exons signify hormone-refractory prostate cancer. Cancer research 2009; 69: 16–22. [PubMed: 19117982]
30. Mu P, Zhang Z, Benelli M, Karthaus WR, Hoover E, Chen CC et al. SOX2 promotes lineage plasticity and antiandrogen resistance in TP53- and RB1-deficient prostate cancer. Science 2017; 355: 84–88. [PubMed: 28059768]
31. Wen Z, Zhong Z, Darnell JE, Jr. Maximal activation of transcription by Stat1 and Stat3 requires both tyrosine and serine phosphorylation. Cell 1995; 82: 241–250. [PubMed: 7543024]
32. Spiotto MT, Chung TD. STAT3 mediates IL-6-induced neuroendocrine differentiation in prostate cancer cells. The Prostate 2000; 42: 186–195. [PubMed: 10639189]
33. Tolomeo M, Cascio A. The Multifaced Role of STAT3 in Cancer and Its Implication for Anticancer Therapy. Int J Mol Sci 2021; 22. [PubMed: 35008458]
34. Neufeld G, Kessler O, Herzog Y. The interaction of Neuropilin-1 and Neuropilin-2 with tyrosine-kinase receptors for VEGF. Adv Exp Med Biol 2002; 515: 81–90. [PubMed: 12613545]
35. Sulpice E, Plouet J, Berge M, Allanic D, Tobelem G, Merkulova-Rainon T. Neuropilin-1 and neuropilin-2 act as coreceptors, potentiating proangiogenic activity. Blood 2008; 111: 2036–2045. [PubMed: 18065694]
36. Hahn D, Simak R, Steiner GE, Handisurya A, Susani M, Marberger M. Expression of the VEGF-receptor Flt-1 in benign, premalignant and malignant prostate tissues. The Journal of urology 2000; 164: 506–510. [PubMed: 10893635]
37. Kaushal V, Mukunyadzi P, Dennis RA, Siegel ER, Johnson DE, Kohli M. Stage-specific characterization of the vascular endothelial growth factor axis in prostate cancer: expression of lymphangiogenic markers is associated with advanced-stage disease. Clinical cancer research : an official journal of the American Association for Cancer Research 2005; 11: 584–593. [PubMed: 15701844]
38. Jackson MW, Roberts JS, Heckford SE, Ricciardelli C, Stahl J, Choong C et al. A potential autocrine role for vascular endothelial growth factor in prostate cancer. Cancer research 2002; 62: 854–859. [PubMed: 11830543]
39. Favier B, Alam A, Barron P, Bonnin J, Laboudie P, Fons P et al. Neuropilin-2 interacts with VEGFR-2 and VEGFR-3 and promotes human endothelial cell survival and migration. Blood 2006; 108: 1243–1250. [PubMed: 16621967]
40. Cai H, Reed RR. Cloning and characterization of neuropilin-1-interacting protein: a PSD-95/Dlg/ZO-1 domain-containing protein that interacts with the cytoplasmic domain of neuropilin-1. J Neurosci 1999; 19: 6519–6527. [PubMed: 10414980]
41. Prahst C, Heroult M, Lanahan AA, Uziel N, Kessler O, Shraga-Heled N et al. Neuropilin-1-VEGFR-2 complexing requires the PDZ-binding domain of neuropilin-1. The Journal of biological chemistry 2008; 283: 25110–25114. [PubMed: 18628209]
42. Ren X, Duan L, He Q, Zhang Z, Zhou Y, Wu D et al. Identification of Niclosamide as a New Small-Molecule Inhibitor of the STAT3 Signaling Pathway. ACS Med Chem Lett 2010; 1: 454–459. [PubMed: 24900231]
43. Szklarczyk D, Morris JH, Cook H, Kuhn M, Wyder S, Simonovic M et al. The STRING database in 2017: quality-controlled protein-protein association networks, made broadly accessible. Nucleic acids research 2017; 45: D362–D368. [PubMed: 27924014]
44. Bishop JL, Thaper D, Vahid S, Davies A, Ketola K, Kuruma H et al. The Master Neural Transcription Factor BRN2 Is an Androgen Receptor-Suppressed Driver of Neuroendocrine Differentiation in Prostate Cancer. Cancer discovery 2017; 7: 54–71. [PubMed: 27784708]
45. Foshay KM, Gallicano GI. Regulation of Sox2 by STAT3 initiates commitment to the neural precursor cell fate. Stem Cells Dev 2008; 17: 269–278. [PubMed: 18447642]
46. Zhu H, Chang LL, Yan FJ, Hu Y, Zeng CM, Zhou TY et al. AKR1C1 Activates STAT3 to Promote the Metastasis of Non-Small Cell Lung Cancer. Theranostics 2018; 8: 676–692. [PubMed: 29344298]

47. Zhao D, Pan C, Sun J, Gilbert C, Drews-Elger K, Azzam DJ et al. VEGF drives cancer-initiating stem cells through VEGFR-2/Stat3 signaling to upregulate Myc and Sox2. Oncogene 2015; 34: 3107–3119. [PubMed: 25151964]

48. Tse BWC, Volpert M, Ratther E, Stylianou N, Nouri M, McGowan K et al. Neuropilin-1 is upregulated in the adaptive response of prostate tumors to androgen-targeted therapies and is prognostic of metastatic progression and patient mortality. Oncogene 2017; 36: 3417–3427. [PubMed: 28092670]

49. Gritsina G, Gao WQ, Yu J. Transcriptional repression by androgen receptor: roles in castration-resistant prostate cancer. Asian journal of andrology 2019; 21: 215–223. [PubMed: 30950412]

50. Liu Y, Horn JL, Banda K, Goodman AZ, Lim Y, Jana S et al. The androgen receptor regulates a druggable translational regulon in advanced prostate cancer. Sci Transl Med 2019; 11.

51. Tam KJ, Dalal K, Hsing M, Cheng CW, Khosravi S, Yenki P et al. Androgen receptor transcriptionally regulates semaphorin 3C in a GATA2-dependent manner. Oncotarget 2017; 8: 9617–9633. [PubMed: 28038451]

52. Lajoie BR, Dekker J, Kaplan N. The Hitchhiker's guide to Hi-C analysis: practical guidelines. Methods 2015; 72: 65–75. [PubMed: 25448293]

53. Khoury A, Achinger-Kawecka J, Bert SA, Smith GC, French HJ, Luu PL et al. Constitutively bound CTCF sites maintain 3D chromatin architecture and long-range epigenetically regulated domains. Nat Commun 2020; 11: 54. [PubMed: 31911579]

54. Taberlay PC, Achinger-Kawecka J, Lun AT, Buske FA, Sabir K, Gould CM et al. Three-dimensional disorganization of the cancer genome occurs coincident with long-range genetic and epigenetic alterations. Genome Res 2016; 26: 719–731. [PubMed: 27053337]

55. Dutta S, Polavaram NS, Islam R, Bhattacharya S, Bodas S, Mayr T et al. Neuropilin-2 regulates androgen-receptor transcriptional activity in advanced prostate cancer. Oncogene 2022; 41: 3747–3760. [PubMed: 35754042]

56. Labrecque MP, Coleman IM, Brown LG, True LD, Kollath L, Lakely B et al. Molecular profiling stratifies diverse phenotypes of treatment-refractory metastatic castration-resistant prostate cancer. J Clin Invest 2019; 129: 4492–4505. [PubMed: 31361600]

57. Giger RJ, Urquhart ER, Gillespie SK, Levengood DV, Ginty DD, Kolodkin AL. Neuropilin-2 is a receptor for semaphorin IV: insight into the structural basis of receptor function and specificity. Neuron 1998; 21: 1079–1092. [PubMed: 9856463]

58. Potiron VA, Sharma G, Nasarre P, Clarhaut JA, Augustin HG, Gemmill RM et al. Semaphorin SEMA3F affects multiple signaling pathways in lung cancer cells. Cancer research 2007; 67: 8708–8715. [PubMed: 17875711]

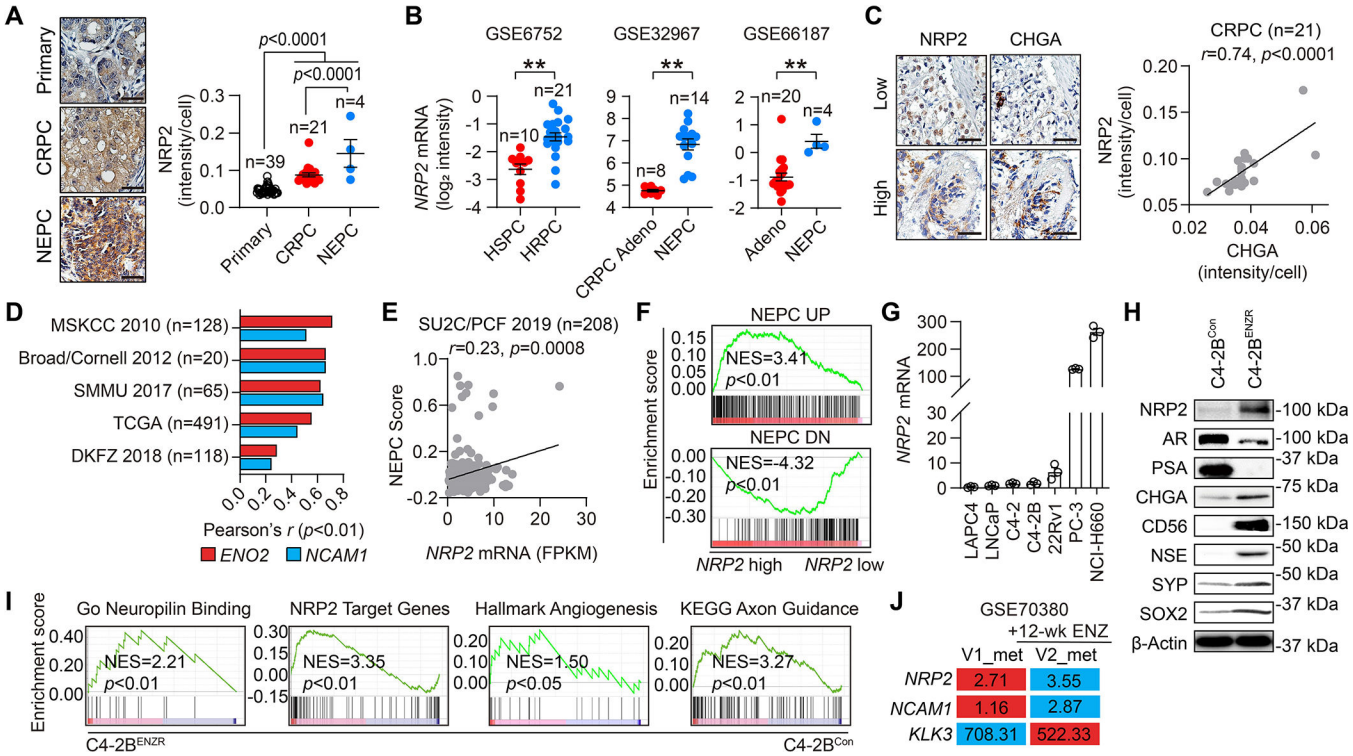

Figure 1. NRP2 expression is upregulated in NEPC.

(A) Representative NRP2 IHC staining and quantification in a PC patient cohort assembling primary PC (n=39), CRPC (n=21) and NEPC (n=4) samples. Scale bars: 250 μm. **(B)** Comparisons of *NRP2* mRNA levels in hormone-sensitive PC (HSPC) versus hormone-refractory PC (HRPC), in CRPC adenocarcinoma (Adeno) versus NEPC, and in prostate adenocarcinoma (Adeno) versus NEPC from the GSE6752, GSE32967 and GSE66197 datasets respectively. **(C)** Representative NRP2 and CHGA IHC staining in serial sections of a CRPC patient tissue microarray (n=21) and corresponding Pearson correlation analysis. Scale bars: 250 μm. **(D)** Pearson correlation analysis of *NRP2* versus *ENO2* and *NCAM1* mRNA in the indicated datasets from the cBioPortal database. **(E)** Pearson correlation analysis of *NRP2* mRNA and NEPC score in the SU2C/PCF 2019 mCRPC cohort from the cBioPortal database. **(F)** GSEA of NEPC gene signatures for the comparisons of *NRP2*-high versus *NRP2*-low patient samples in the TCGA primary PC cohort. **(G)** qPCR of *NRP2* in a panel of indicated human PC cell lines (n=3). **(H)** Western blot of NRP2 and other indicated proteins in control and ENZ^{R} C4–2B cells. **(I)** GSEA of the indicated gene signatures for the comparisons of ENZ^{R} versus control C4–2B cells. **(J)** *NRP2, KLK3* and *NCAM1* mRNA levels (unit: RPKM) in the RNA-seq dataset GSE70380. V1_met: rib metastasis obtained during first visit and before treatment; V2_met: metastasis obtained during second visit after ENZ treatment for 12 weeks. Data represent the mean ± SEM. ** p<0.01.

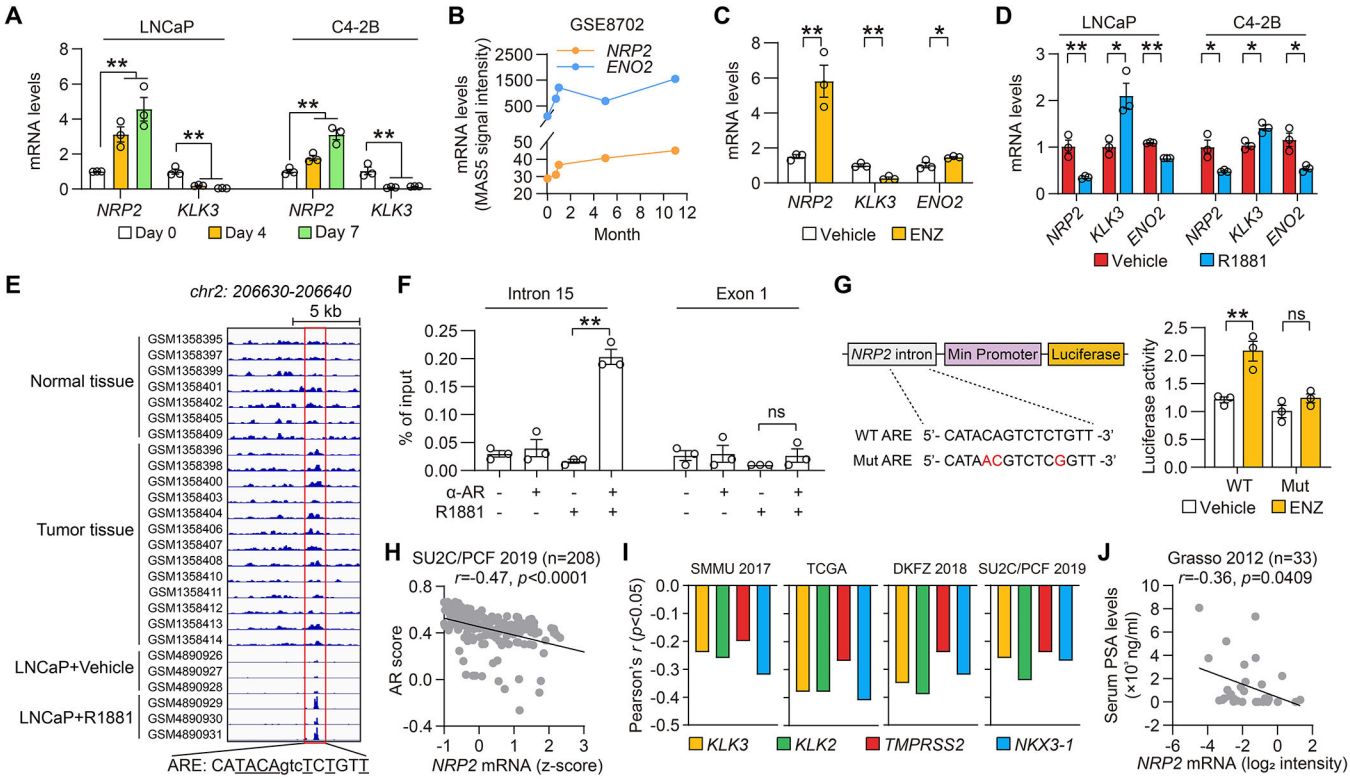

Figure 2. NRP2 is transcriptionally repressed by AR.

(A) qPCR of *NRP2* and *KLK3* in LNCaP and C4–2B cells upon ENZ treatment (10 μM) for the indicated times (n=3). **(B)** *NRP2* mRNA levels (unit: MAS5 normalized intensity) in LNCaP cells exposed to long-term culture in androgen-deprived medium from the RNA-seq dataset GSE8702. **(C)** qPCR of *NRP2, KLK3* and *ENO2* in LNCaP cells treated with ENZ (10 μM, 6 hours) (n=3). **(D)** qPCR of *NRP2, KLK3* and *ENO2* in LNCaP and C4–2B cells upon R1881 stimulation (10 nM, 6 hours) (n=3). **(E)** Genomic browser representation of AR binding in *NRP2* intron 15 encompassing an ARE, with the nucleotides identical to the canonical ARE underlined, in the GSE161167 (LNCaP cells) and GSE70079 (a cohort of normal and tumor human prostate tissues) datasets. **(F)** ChIP-qPCR of AR occupancy at sequences of the *NRP2* ARE-centric intron 15 and exon 1 by R1881 (10 nM, 24 hours) in LNCaP cells. Data represent the percent of input (n=3). **(G)** Determination of *NRP2* ARE-luc activity in WT or mutated forms by ENZ (10 μM, 6 hours) in LNCaP cells (n=3). Schematic of WT and mutated *NRP2* ARE-luc, with nucleotides selected for mutations in red, is shown separately. **(H)** Pearson correlation analysis of *NRP2* mRNA and AR score in the SU2C/PCF 2019 mCRPC cohort. **(I)** Pearson correlation analysis of *NRP2* versus *KLK3, KLK2, TMPRSS2* and *NKX3–1* mRNA in the indicated datasets from the cBioPortal database. **(J)** Pearson correlation analysis of *NRP2* mRNA with serum PSA levels in the Grasso dataset from the Oncomine database. Data represent the mean ± SEM. **p*<0.05, ***p*<0.01; ns, not significant.

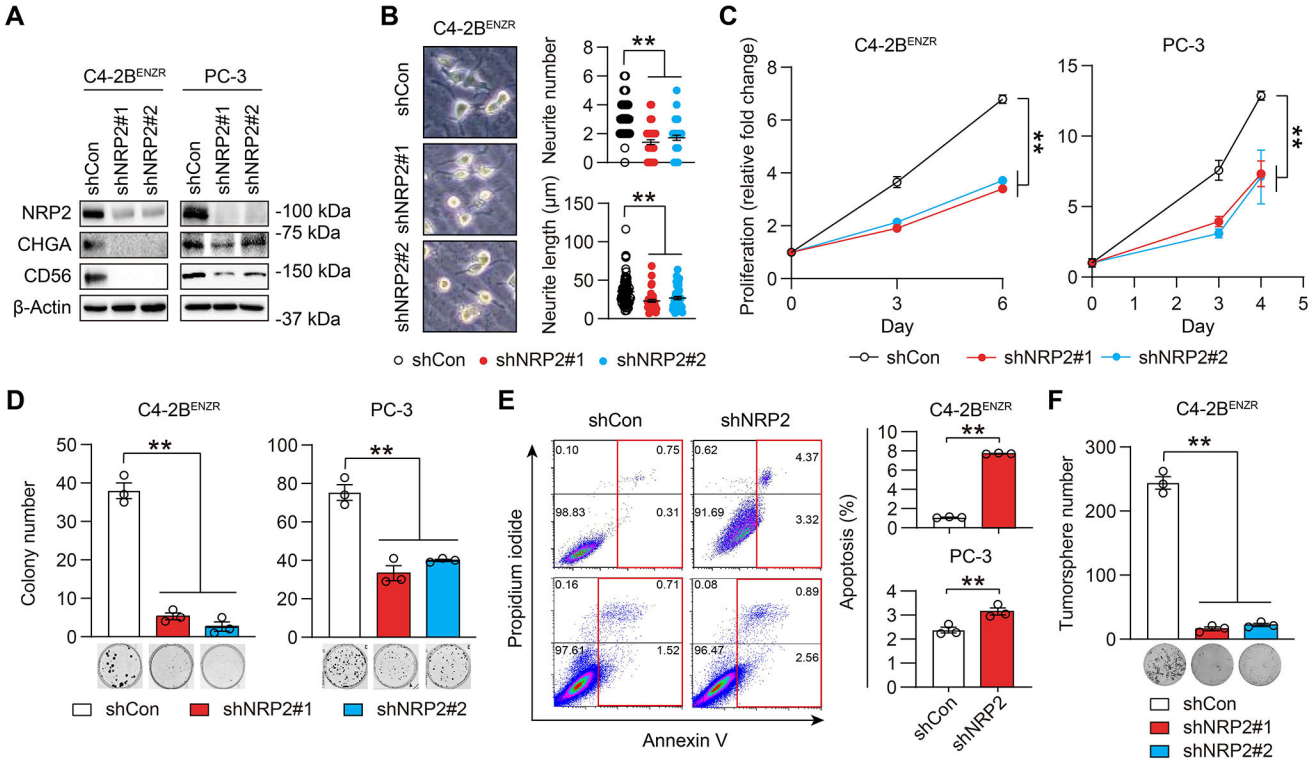

Figure 3. Knockdown of NRP2 represses the NE traits and aggressive behavior of NEPC cells.

(A) Western blot of NRP2, CHGA and CD56 in control and NRP2-knockdown C4–2B^{ENZR} and PC-3 cells. **(B)** Representative images of control and NRP2-knockdown C4–2B^{ENZR} cell morphology and corresponding quantification of per-cell number of neurites and average neurite length in each group (n=50 cells/group), as a representative of 3 independent experiments. **(C)** MTS cell proliferation assays of control and NRP2-knockdown C4–2B^{ENZR} and PC-3 cells. Data represent the fold changes of cell proliferation during an observation period of up to 6 days (n=3). Fold change on the day of cell seeding (day 0) in each group was set as 1. **(D)** Representative images and quantification of colonies formed in control and NRP2-knockdown C4–2B^{ENZR} and PC-3 cells (n=3). **(E)** Flow cytometric analysis of cell apoptosis by the percent of Annexin V^{+} cell populations in control and NRP2-knockdown C4–2B^{ENZR} and PC-3 cells (n=3). **(F)** Representative images and quantification of tumorspheres formed by control and NRP2-knockdown C4–2B^{ENZR} cells (n=3). Data represent the mean ± SEM. $^{**}p<0.01$.

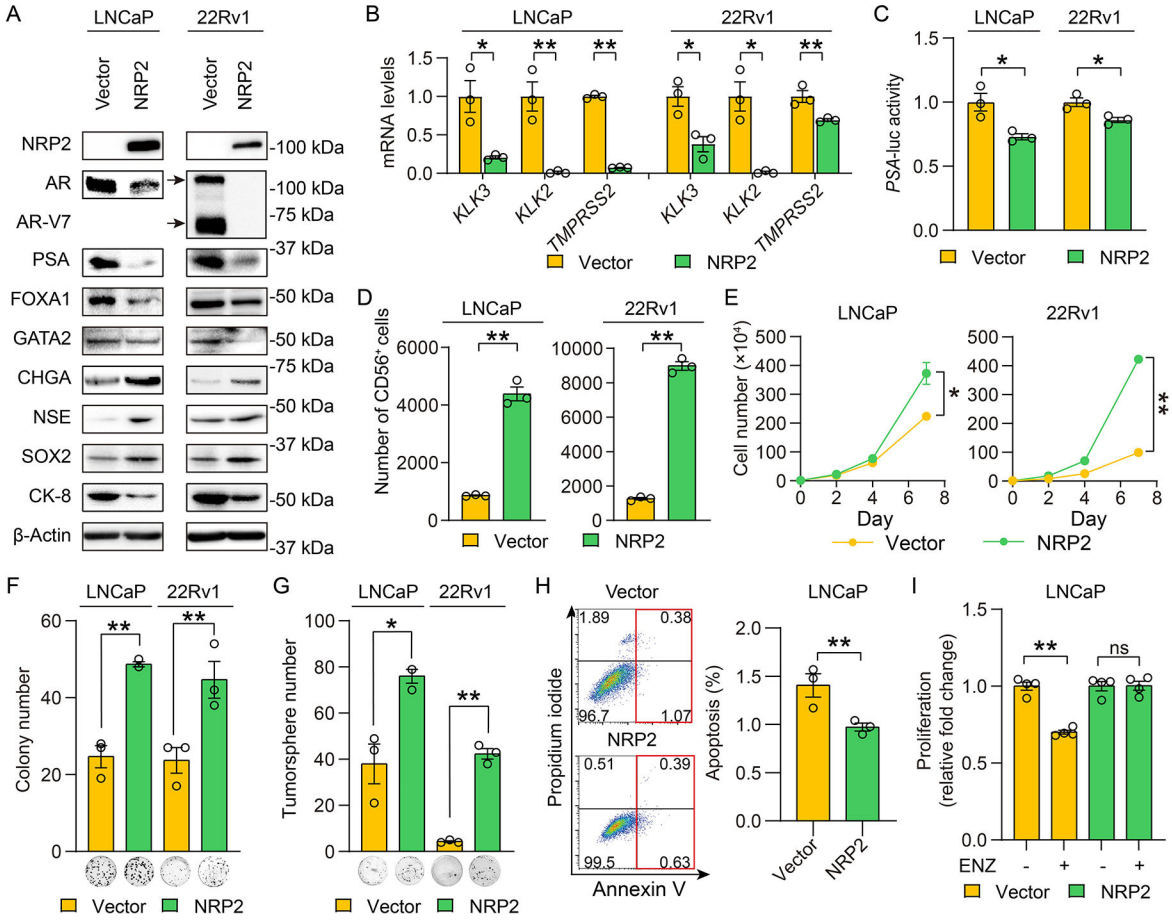

Figure 4. NRP2 overexpression attenuates AR signaling and promotes NE plasticity and PC cell aggressiveness.

(A) Western blot of indicated proteins in control and NRP2-overexpressing LNCaP and 22Rv1 cells. **(B)** qPCR of the indicated AR target genes in control and NRP2-overexpressing LNCaP and 22Rv1 cells (n=3). **(C)** Determination of *PSA*-luc activity in control and NRP2-overexpressing LNCaP and 22Rv1 cells (n=3). **(D)** Flow cytometric quantification of $CD56^+$ cells per 50,000 cells in control and NRP2-overexpressing LNCaP and 22Rv1 cells (n=3). **(E)** Cell counting assays of control and NRP2-overexpressing LNCaP and 22Rv1 cells in a 7-day observation period (n=3). **(F, G)** Representative images and quantification of colonies (F) and tumorspheres (G) formed by control and NRP2-overexpressing LNCaP and 22Rv1 cells (n=3). **(H)** Flow cytometric analysis of cell apoptosis by the percent of Annexin V^+ cell populations in control and NRP2-overexpressing LNCaP cells (n=3). **(I)** MTS cell proliferation assays of control and NRP2-overexpressing LNCaP cells upon ENZ treatment (5 μM, 5 days). Data represent the fold changes of cell proliferation on day 5 relative to cell seeding day (day 0) (n=4), with fold changes in non-treated groups set as 1 for normalization of paired treated groups. Data represent the mean ± SEM. *p<0.05, **p<0.01; ns, not significant.

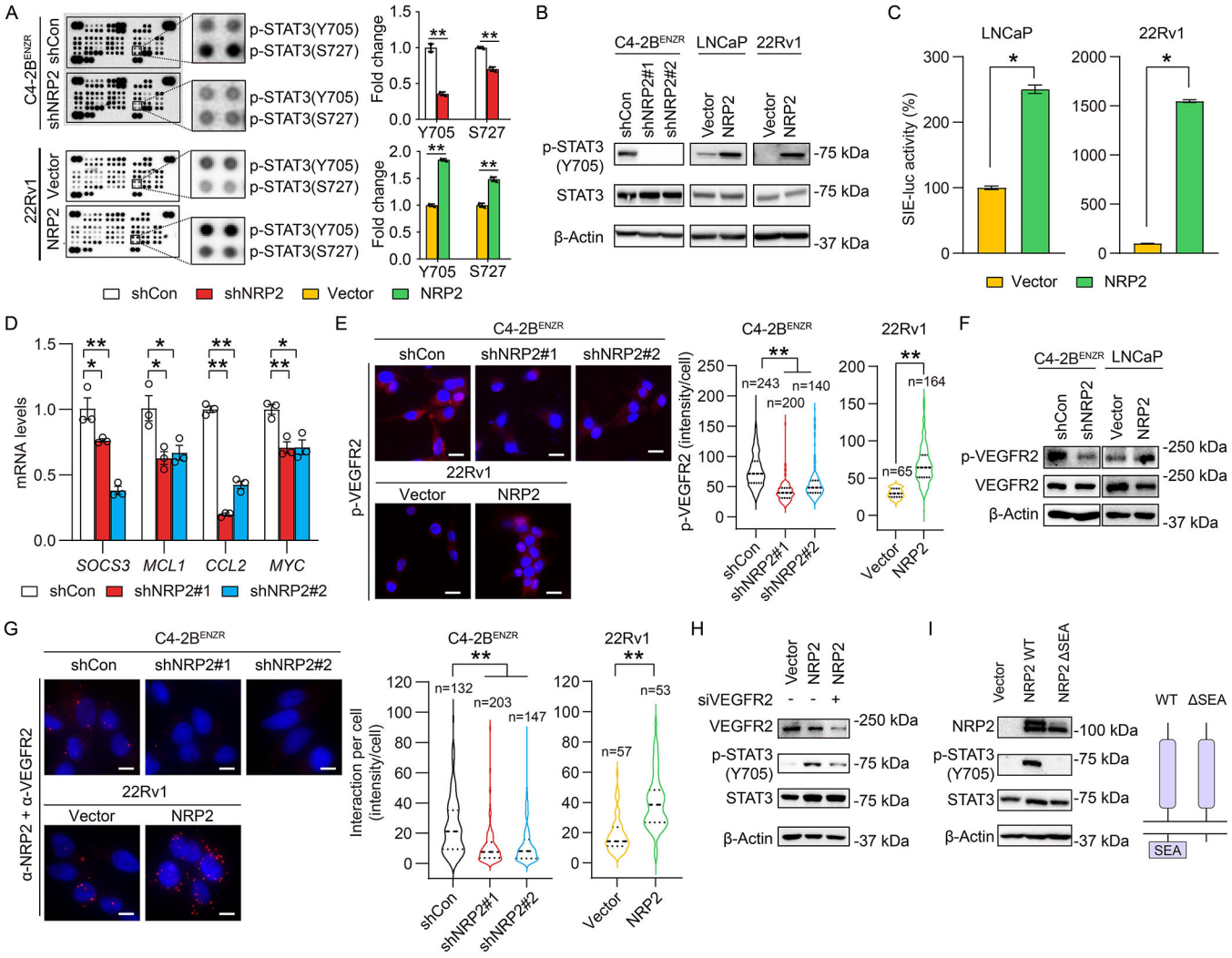

Figure 5. NRP2 activates STAT3 in a VEGFR2-dependent manner.

(A) Representative images of phospho-kinase antibody array and quantification of p-STAT3 levels from indicated cells. **(B)** Western blot of p-STAT3 (Y705) and STAT3 in indicated cells. **(C)** Determination of STAT3-responsive SIE-luc activity in control and NRP2-overexpressing LNCaP and 22Rv1 cells (n=3). **(D)** qPCR of the indicated STAT3 target genes in control and NRP2-knockdown C4–2B^{ENZR} cells (n=3). **(E)** Representative p-VEGFR2 immunofluorescence staining and quantification in indicated cells cultured in the presence of only endogenous ligands. Scale bars: 50 μm. **(F)** Western blot of p-VEGFR2 and VEGFR2 in indicated cells cultured in the presence of only endogenous ligands. **(G)** Representative PLA staining and quantification of NRP2-VEGFR2 interaction in the cytoplasm of indicated cells. Scale bars: 30 μm. **(H)** Western blot of p-STAT3 (Y705) and STAT3 in control and NRP2-overexpressing 22Rv1 cells upon siRNA-mediated VEGFR2 knockdown. **(I)** Western blot of p-STAT3 (Y705) and STAT3 in 22Rv1 cells transiently expressing WT NRP2 or a mutant form of NRP2 lacking cytoplasmic SEA motif (NRP2-ΔSEA). Schematic of full-length WT NRP2 and NRP2-ΔSEA is shown separately. Data represent the mean ± SEM. *p<0.05, **p<0.01.

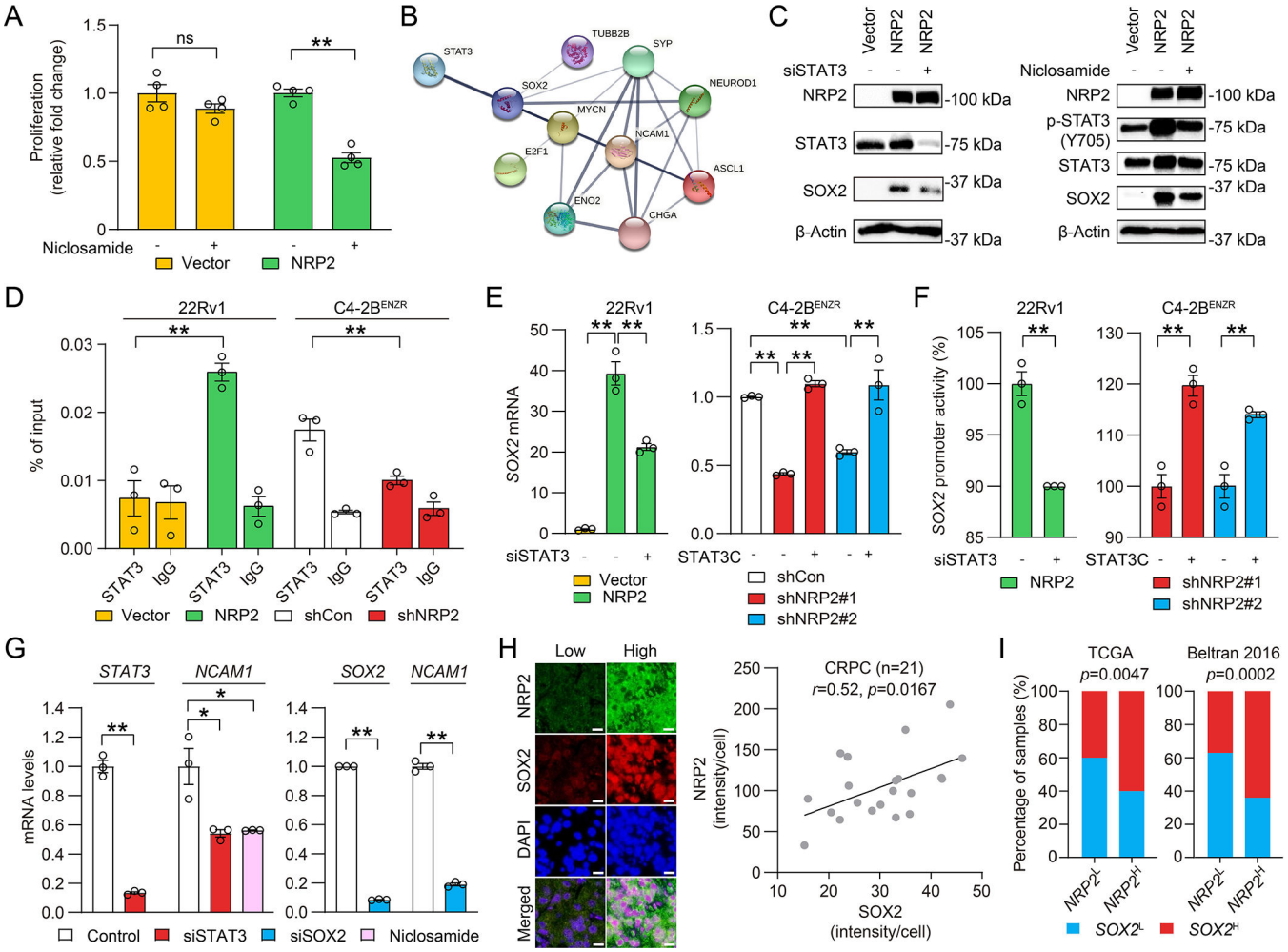

Figure 6. NRP2 induces NE plasticity and NEPC cell growth by STAT3 and SOX2.

(A) MTS cell proliferation assays of NRP2-overexpressing LNCaP cells upon niclosamide (1 μM, 5 days) treatment. Data represent the fold changes of cell proliferation on day 5 relative to cell seeding day (day 0) (n=4), with fold changes in non-treated groups set as 1 for normalization of paired treated groups. **(B)** STRING analysis of a PC NE gene signature for linking with STAT3 via SOX2. **(C)** Western blot of p-STAT3 (Y705), STAT3 and SOX2 in control and NRP2-overexpressing 22Rv1 cells upon treatment with STAT3 siRNA or niclosamide (20 μM, 12 hours). **(D)** ChIP-qPCR of STAT3 occupancy at a STAT3-binding *SOX2* promoter region in indicated cells. Data represent the percent of input (n=3). **(E)** qPCR of *SOX2* in control and NRP2-overexpressing 22Rv1 cells upon *STAT3* siRNA treatment, and in control and NRP2-knockdown C4–2B^{ENZR} cells expressing STAT3C, a constitutively active form of STAT3 (n=3). **(F)** Determination of *SOX2* promoter activity in NRP2-overexpressing 22Rv1 cells under *STAT3* siRNA treatment, and in NRP2-knockdown C4–2B^{ENZR} cells expressing STAT3C (n=3). **(G)** qPCR of *STAT3*, *SOX2* and *NCAM1* in 22Rv1 cells treated with *STAT3* or *SOX2* siRNAs or niclosamide (20 μM, 12 hours) (n=3). **(H)** Representative NRP2 and SOX2 double quantum dot staining and corresponding Pearson correlation analysis in a CRPC patient tissue microarray (n=21). Scale bars: 50 μm. **(I)** Chi-Square analysis of distribution of *SOX2* mRNA levels (L, low; H, high) in

NRP2-low and -high groups from the TCGA and Beltran 2016 CRPC/NEPC cohorts at cBioPortal. Data represent the mean ± SEM. *p<0.05, **p<0.01; ns, not significant.

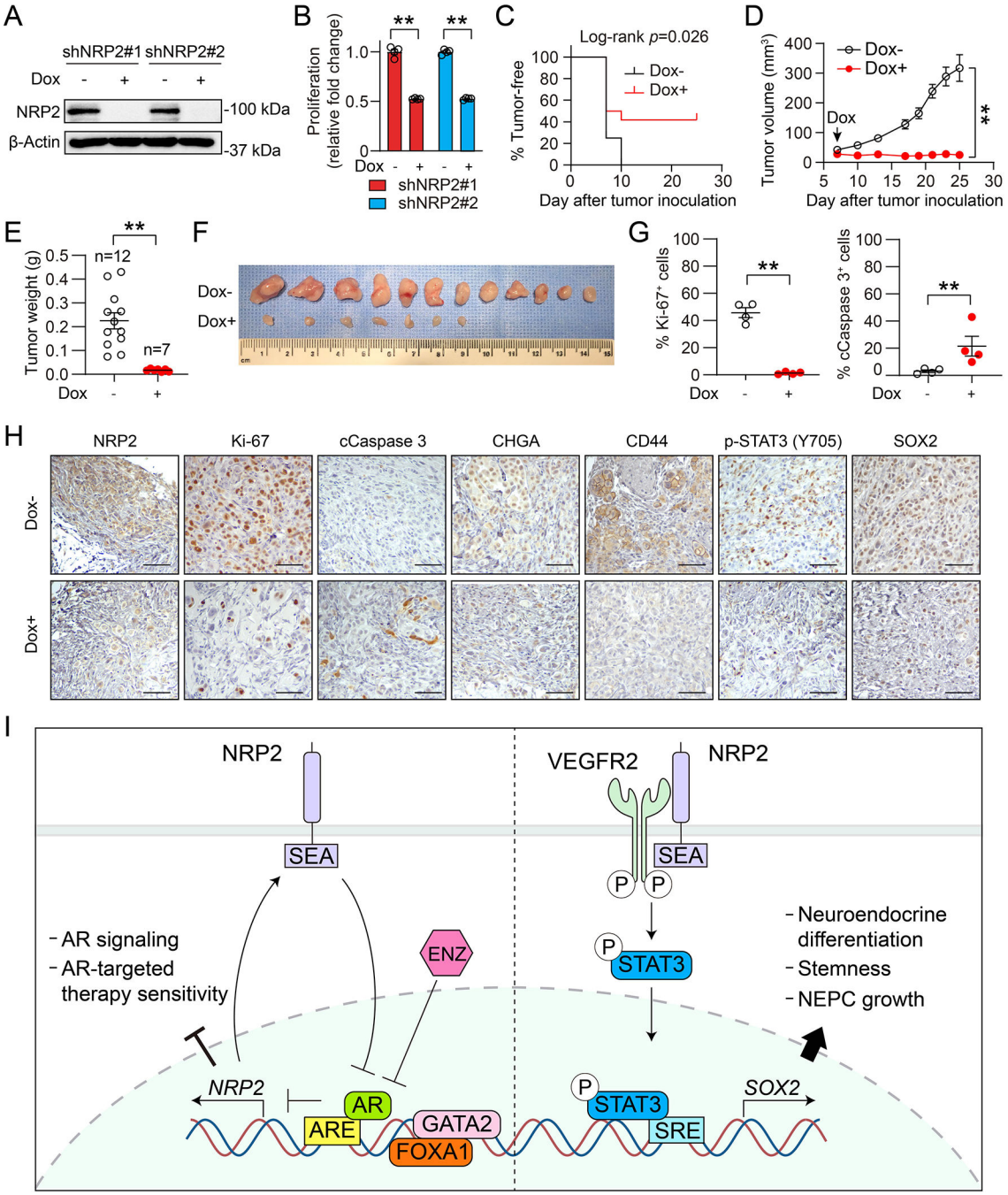

Figure 7. NRP2 silencing restricts NEPC tumor growth in mice.

(A) Western blot of NRP2 in PC-3 cells expressing Dox-inducible *NRP2* shRNAs upon Dox stimulation (100 ng/ml, 3 days). **(B)** MTS cell proliferation assays of PC-3 cells expressing Dox-inducible *NRP2* shRNAs upon Dox stimulation (100 ng/ml, 3 days). Data represent the fold changes of cell proliferation on day 3 relative to cell seeding day (day 0) (n=4), with fold changes in non-treated groups set as 1 for normalization of paired treated groups. **(C)** Kaplan-Meier tumor-free curves of mice inoculated with PC-3 cells expressing a Dox-inducible *NRP2* shRNA (shNRP2#1) and fed a Dox- or a Dox+ diet

(n=12 injection points per group). **(D)** PC-3 tumor growth curves of mice fed a Dox− or a Dox+ diet (Dox−, n=12; Dox+, n=7). **(E, F)** PC-3 tumor weights (E) and anatomic tumor images (F) at the endpoint. **(G)** Quantification of % of Ki-67^{+} and cleaved caspase 3^{+} cells in PC-3 tumor samples (n=4). **(H)** Representative IHC staining of NRP2, Ki-67, cleaved caspase 3, CHGA, CD44, p-STAT3 (Y705) and SOX2 in tumor samples. Scale bars: 200 μm. **(I)** Schematic summarizing the mechanism by which NRP2 promotes NEPC, where upregulation of NRP2, upon relieving AR transcriptional repression under ADT (e.g., ENZ), suppresses AR signaling and activates the VEGFR2/STAT3/SOX2 pathway to induce NE plasticity and drive NEPC cell growth. Data represent the mean ± SEM. $^{**}p<0.01$.